Reaction-Diffusion-Maniolds for Flame-Wall-Interactions of Stratified Flames

Christina Strassacker, Viatcheslav Bykov, Ulrich Maas
Karlsruhe Institute of Technology, Institute of Technical Thermodynamics
Engelbert-Arndold-Strasse 4, Karlsruhe 76131, Germany

1 Introduction

Combustion processes close to walls represent an enormous challenge in combustion science and technology. Therefore, today's research focuses on so-called Flame-Wall-Interactions (FWI) in order to understand and to model the thermo-chemical processes. Previous numerical and experimental investigations regarding flame wall interactions focused on completely premixed flames. However, modern engines typically do not operate with premixed mixtures, but operate in stratified flame regimes. This leads to the demand for investigations that are closer to reality which means that inhomogeneous mixtures need to be considered.

In order to study combustion systems numerically, the use of reduced kinetic models is useful to keep the computation time low and feasible for numerical integration. One type of these reduced kinetic models are manifold based reduced kinetic models [1–7] like flamelets based methodologies [3], the Flamelet Generated Manifold (FGM) [4], the flame prolongation of ILDM (FPI) [5], the ILDM [6] and the so–called Reaction-Diffusion-Manifold (REDIM) [7].

In this study, the REDIM method is applied. In previous works regarding flame-wall-interactions with the REDIM method [8, 9], two-dimensional REDIMs for laminar flat and premixed flames of homogeneous mixtures were generated. In order to enable accurate reduced computations for practically relevant combustion regimes, an approach that allows the construction of a REDIM that is able to handle stratified flames with flame-wall-interactions is proposed in this work. It is possible to recapture those scenarios within the REDIM method, but here, a two-dimensional REDIM is not sufficient. This is due to the fact, that the thermo-chemical states of these flames are not always part of the same two-dimensional subspace, but they are part of higher-dimensional subspaces, especially for computations with different starting solutions (slight change in mixture compositions at the different locations in the computational domain). Therefore, the dimension must be increased and three-dimensional REDIMs are generated. An approach to construct these REDIMs is suggested and demonstrated in this work and different three-dimensional REDIMs are constructed and compared to each other afterwards.

Correspondence to: christina.strassacker@kit.edu

2 Reaction-Diffusion Manifolds for stratified flame-wall-interactions

The REDIM method is a method to devise a reduced kinetic model that accounts for both chemical reaction and molecular transport. The reduction method is based on the assumption, that only the time scales of a few reactive and diffusive processes overlap and need to be accounted for. This defines the reduced model dimension [7, 10, 11].

Before the REDIM evolution equation can be solved, an initial guess as well as a gradient estimate need to be specified [7]. The initial guess for stratified flames with FWI is generated by merging several initial guesses for different homogeneous mixture compositions. Each of these initial guesses is constructed via detailed sample solutions of the model configuration. This model configuration has been studied in a number of previous works regarding FWI with the REDIM method [8, 9, 12]. A premixed methane/air flame travels towards a wall and extinguishes due to heat losses. The equivalence ratio ϕ of the premixed gases is varied from $\phi = 0.5$ to $\phi = 2.0$. For the numerical treatment, the reacting flow solver INSFLA [13] is used to study the one-dimensional problem. For the modelling of the molecular diffusion, equal diffusivities and the assumption of unity Lewis-Number are assumed for simplicity. The use of more sophisticated transport models in the context of the REDIM is possible without any principle difficulties (see e.g. [8, 9, 14]). The initial guesses of the two-dimensional REDIMs of different mixtures are parametrized with the specific enthalpy and the specific mole number of $\mathrm{CO_2}$ (see Fig. 1(b)). Afterwards, those two-dimensional initial guesses are combined, and a three-dimensional initial guess is built (see Fig. 1(b)). Due to the differing mixture compositions, the amount of $\mathrm{N_2}$ of the different initial guesses varies wherefore $\mathrm{N_2}$ can be taken as third parametrization variable.

The specification of a gradient estimate is comparable to the definition of a scalar dissipation rate of a flamelet generated manifold even if its influence is less than in the case of an FGM. Both the scalar dissipation rate as well as the gradient estimate are responsible for diffusive processes and therefore, the manifold should be able to recapture the relevant processes of the transport.

In this work, the gradient estimate is partly used from detailed sample solutions: a three-dimensional REDIM is generated and the gradient estimate of three different state variables that represent the coupling of chemical reaction and molecular diffusion of the combustion system need to be specified. For the specification of the heat loss at the wall and the progress of the chemical reaction, the gradient estimate of the specific enthalpy as well as the gradient estimate of the specific mole number of $\mathrm{CO_2}$ are used. Different from REDIMs for homogeneous mixtures, a gradient estimate that represents the mixing process needs to be specified. For this purpose, a gradient estimate of $\mathrm{N_2}$ is used, because the value of $\mathrm{N_2}$ changes for the different mixture compositions. The spatial gradient of the detailed sample solution of $\mathrm{N_2}$ is not suitable in this case because the detailed sample solutions were obtained with homogeneous mixtures and the gradient estimate would not represent the mixing between the different mixture compositions.

In order to find a representative value for the gradient estimate and to provide a solution, counterflow calculations that represent the mixing of a stoichiometric mixture and a mixture with $\phi = 0.75$ are performed for strain rates $a = \sqrt{J/\rho}$ of a wide range to cover cases which might occur in practical applications ($95s^{-1}$ - $950s^{-1}$) with the tangential pressure gradient $J = 1/r\partial p/\partial r$ [15] (see exemplarily Fig. 1(a) with the strain rate $a \approx 104s^{-1}$). It is figured out, that the magnitude of the value of the spatial gradient of $\mathrm{N_2}$ is nearly the same or even very similar as the one of $\mathrm{CO_2}$. Therefore, by using this similarity, the gradient estimate

$$\frac{\partial \mathrm{N_2}}{\partial x} = -\frac{\partial \mathrm{CO_2}}{\partial x} \tag{1}$$

is used for the third dimension.

As it was mentioned above, in order to investigate the system in more detail and to reduce the computational

Table 1: Generation of the different gradient estimates. Stars * indicate that the gradient estimate was generated by detailed sample solutions.

	$\phi = 0.5$	$\phi = 0.75$	$\phi = 1.0$	$\phi = 1.25$	$\phi = 1.5$	$\phi = 1.75$	$\phi = 2.0$
REDIM_1	*	*	*	*	*	*	*
REDIM_2	*	interpolated	*	interpolated	*	interpolated	*
REDIM_3	*	interpolated	*	interpolated	interpolated	interpolated	*

effort before the generation of the REDIM, the gradient estimates of some layers are not taken from the detailed sample solution of the specific mixture compositions, but they are linearly interpolated by the gradient estimates of other mixture composition (see Tab. 1). In this way, for example the gradient estimate of $\phi = 0.75$ for REDIM_2 is generated by interpolating it with the grids of $\phi = 0.5$ and $\phi = 1.0$. Therefore, three REDIMs (REDIM_1, REDIM_2 and REDIM_3) with differing gradient estimates are generated, starting from the same initial guess.

For the validation of the REDIMs with gradient estimates of different levels of detail, an additional REDIM with a varied number of grid points is generated. This REDIM (REDIM_4) is generated with half of the number of grid points in every direction and a detailed gradient estimate. Therefore, this REDIM serves as reference value for the occurring error that is caused using the interpolated gradient estimate in REDIM_2. and REDIM_3 because with this REDIM, the error occurring due to the discretization of the REDIMs can be quantified.

The REDIM evolution equation is applied for the different meshes. At the boundaries of the REDIM, that do not correspond to boundaries in physical space, boundary conditions that allow the REDIM to evolve are applied [16]. At boundaries of the REDIM, that correspond to boundaries in physical space, Dirichlet boundary conditions are used. In the following, the different REDIMs are compared to each other.

3 Comparison of the different REDIMs

For the comparison of the different REDIMs, the states of the REDIMs at the grid points are investigated where the differences between the manifolds are measured by

$$\delta = \left|\left| P_1 \cdot (\Psi_{\mathrm{REDIM}_1} - \Psi_{\mathrm{REDIM_i}}) \right|\right| \tag{2}$$

where Ψ is the state vector, $P_1 = (\Psi_\theta^T \cdot \boldsymbol{S} \cdot \Psi_\theta)^{-1} \cdot \Psi_\theta^T \cdot \boldsymbol{S}$ is the local projection onto the normal space of REDIM_1, $\left|\left|...\right|\right|$ is the euclidean norm and $i = 2, ...4$. Here, Ψ_θ is the matrix of partial derivatives of Ψ with respect to the generalized coordinates θ that spans the tangential subspace of the REDIM.

In order to overcome problems with different scales of the thermokinetic variables, the projection operator P_1 is scaled with the diagonal scaling matrix $\boldsymbol{S} = diag(10^{-12}, 10^{-12}, 1, ..., 1)$ to scale the enthalpy and pressure to values of the order 1. For the computation of δ for REDIM_4, only the grid points of REDIM_1 that correspond to the ones of REDIM_4 are used (half of the grid points in each direction are dropped).

In this way, the distance δ is nondimensionalized and the differences of enthalpy h, pressure p and the species can be summed up. Thus, the vector between the grid points of the two REDIMs is projected at any grid point onto the normal subspace of the manifold and the distance δ is then given by the norm of this projection.

Figure 1(c) shows the normed distances of REDIM_1 and REDIM_2 as well as the normed distances of

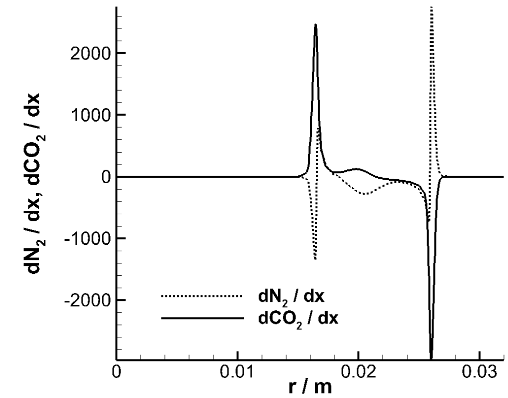

(a) Spatial gradients of the specific mole number of N_2 (dashed line) and CO_2 (solid line) of the counterflow configuration for the strain rate $a \approx 104s^{-1}$ with different air-fuel-ratios.

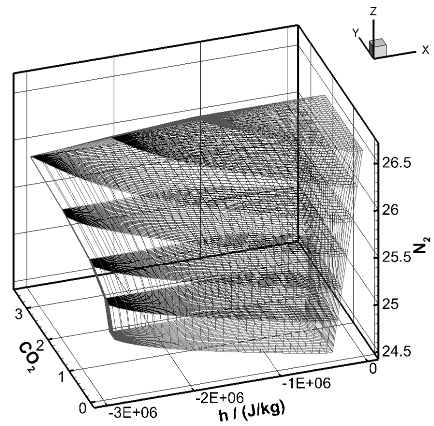

(b) Two-dimensional initial meshes for the different air-fuel ratios (black) and the three-dimensional initial mesh of REDIM_1, REDIM_2 and REDIM_3 (grey; only the boundary cell faces are illustrated for brevity).

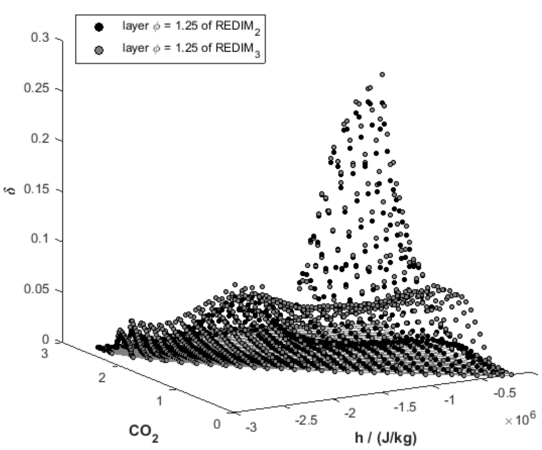

(c) Normed distances δ between the states of two different layers of (a) REDIM_1 and REDIM_2 and (b) REDIM_1 and REDIM_3; only the layers with the largest distance are shown for brevity.

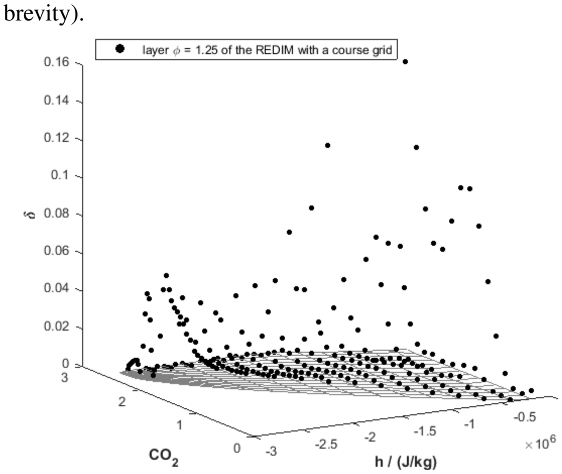

(d) Normed distances δ between the states of two different layers of REDIM_1 and REDIM_4.

Figure 1: Spatial gradients of CO_2 and N_2, meshes for the generation of the three-dimensional initial guesses and normed distance δ between the states of two different layers of the REDIMs.

REDIM_1 and REDIM_3 at all grid points. For a better clarity, only the layers of the largest distance in every case is illustrated. As one may expect, layers that were interpolated show the largest distances δ, namely the layer of $\phi = 1.25$. For all other layers except the layer of $\phi = 1.5$ of REDIM_3, the distance is approximately one fifth or less than the illustrated ones. Moreover, it can be observed, that the distances for REDIM_2 and REDIM_3 compared to REDIM_1 are nearly the same although the gradient estimate of REDIM_3 is coarser than the one of REDIM_2.

Figure 1(d) shows the normed distances of REDIM_1 and REDIM_4 at all grid points of REDIM_4 for the

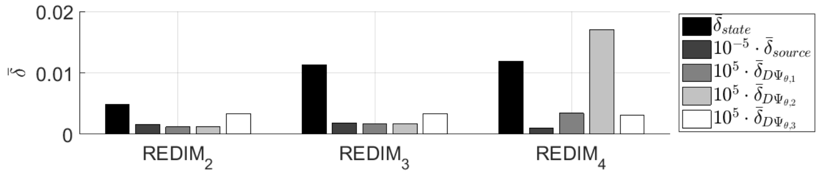

Figure 2: Overall grid points averaged distance $\bar{\bar{\delta}}$ of the states, the source term and the diffusive terms.

layer of $\phi = 1.25$. It can be observed, that the maximum distances for this layer are smaller than the maximum distances of REDIM_2 and REDIM_3. In the case depicted in Fig. 1(d), the distances of most layers which are not illustrated are of the same magnitude or partly on the REDIM even higher than the illustrated one.
Figure 2 shows the overall grid points averaged distance of REDIM_1 from REDIM_2, REDIM_3 and REDIM_4 not only for the states but also for the source term as well as the diffusive term $D \cdot \Psi_\theta$ at the given grid points. Therefore, Eq. 2 is applied for the source term as well as for the diffusive term $D \cdot \Psi_\theta$ which is computed during the REDIM integration [7]. The averaged distance of the states of REDIM_2 is less than the averaged distance of the states of REDIM_4. The averaged distance of the states of REDIM_3 is of the same magnitude than the averaged distance of the states of REDIM_4. The distances are relatively small compared to the actual values of the states. Therefore, here the relative errors are very small. The same trend can be observed for the normed and overall grid points averaged distance of the source term as well as for the diffusion terms which are responsible for the system dynamic of the combustion process.
This means, that the occurring error due to a rough gradient estimate is of an acceptable magnitude, namely the same or even less than the occurring error due to discretization. Therefore, the use of REDIM_2 or REDIM_3 instead of REDIM_1 or REDIM_4 with the exact gradient estimate seems to be reasonable because the occurring error during reduced computations is of the same magnitude.
Although this low dependence on the gradient estimate was shown in particular for the REDIM method, it has also consequences for other reduction methods or analyses of reacting flows, which are in accordance with finding from correlation analyses of DNS data: The actually accessed thermokinetic states in a reacting flow depend only slightly on the local gradients.

5 Conclusion

In this work, the REDIM method was applied to the thermokinetic state of stratified flames with flame-wall-interactions. Therefore, different strategies were suggested, implemented and verified. The initial guesses were generated by merging several initial guesses for different mixture compositions. According to the mixing between the different mixture compositions, the gradient estimate of N_2 is changed compared to the gradient estimates for the other dimensions. In order to verify the approach, two further gradient estimates which were interpolated are analyzed and compared to a REDIM with a course grid. In these cases, not all the detailed computations of the combustion system for each mixture composition are necessary. It was figured out, that the REDIMs with only rough gradient estimate are very similar to the REDIM with a detailed gradient estimate, there are only slight differences between the REDIMs which are in the same magnitude than the differences between the fine and course grid and detailed gradient estimate. These differences can be neglected, especially in turbulent combustion regimes.
While the result of a weak dependence of the low dimensional manifolds on the local gradients was shown

in particular for the REDIM method, it has also consequences for other reduction methods or analyses of reacting flows: It shows, that the actually accessed thermokinetic states in a reacting flow depend only weakly on the local gradients. This is a result, which is in accordance with finding from correlation analyses of DNS data.

Acknowledgments

This research was supported by the Deutsche Forschungsgemeinschaft (DFG) within the SFB/Transregio 150.

References

[1] Fenichel N. (1979). Geometric singular perturbation theory for ordinary differential equations. Journal of differential equations 31: 53-98.
[2] Pope SB, Maas U. (1993). Simplifying chemical kinetics: Trajectory-generated low-dimensional manifolds. Mechanical and Aerospace Engineering Report: FDA, 11.
[3] Coelho PJ, Peters N. (2001). Unsteady modelling of a piloted methane/air jet flame based on the Eulerian particle flamelet model. Combust. Flame 124(3): 444-465.
[4] Nguyen PD, Subramanian V, Domingo P, Vervisch L. (2009). Multidimensional Flamelet Manifolds for hybrid combustion regimes. 4th European Combustion Meeting, Vienna.
[5] Gicquel O, Darabiha N, Thévenin D. (2000). Liminar premixed hydrogen/air counterflow flame simulations using flame prolongation of ILDM with differential diffusion. Proc. Combust. Inst. 28(2): 1901-1908.
[6] Maas U, Pope SB. (1992). Simplifying chemical kinetics: intrinsic low-dimensional manifolds in composition space. Combust. Flame 88(3-4): 239-264.
[7] Bykov V, Maas U. (2007). The extension of the ILDM concept to reaction–diffusion manifolds. Combust. Theory and Modelling 11(6): 839-862.
[8] Strassacker C, Bykov V, Maas U. (2018). REDIM reduced modeling of flame quenching at a cold wall–The influence of detailed transport models and detailed mechanisms. Comb. Sci. and Technol.: 1-15.
[9] Strassacker C, Bykov V, Maas U. (2018). REDIM reduced modeling of quenching at a cold wall including heterogeneous wall reactions. Internat. Journal of Heat and Fluid Flow 69: 185-193.
[10] Bykov V, Maas U. (2009). Problem adapted reduced models based on Reaction–Diffusion Manifolds (REDIMs). Proc. Combust. Inst. 32: 561-568.
[11] Bykov V, Maas U. (2011) An Analysis of the Attractive Properties of REDIM Manifolds for Model Reduction. Proc. Internat. Colloqu. on Dynamics of Explosions and Reactive Systems 23:198,24-29.
[12] Steinhilber G, Bykov V, Maas U.(2017). REDIM reduced modeling of FWI: Quenching of a premixed methane/air flame at a cold inert wall.Proc. Combust. Inst. 36:655-661.
[13] Maas U, Warnatz J. (1988). Ignition processes in hydrogen-oxygen mixtures. Combust. Flame 74: 53-69.
[14] Maas U, Bykov V. (2011). The extension of the reaction/diffusion manifold concept to systems with detailed transport models. Proc. Combust. Inst.33: 1253-1259.
[15] Stahl G, Warnatz J. (1991). Numerical investigation of time-dependent properties and extinction of strained methane and propane-air flamelets. Combust. Flame 85(3-4): 285-299.
[16] Neagos A, Bykov V, Maas U. (2017). Adaptive hierarchical construction of reaction–diffusion manifolds for simplified chemical kinetics. Proc. Combust. Inst. 36: 663-672.